

© 2021. M. Chalecki, G. Jemielita.

This is an open-access article distributed under the terms of the Creative Commons Attribution-NonCommercial-NoDerivatives License (CC BY-NC-ND 4.0, <https://creativecommons.org/licenses/by-nc-nd/4.0/>), which permits use, distribution, and reproduction in any medium, provided that the Article is properly cited, the use is non-commercial, and no modifications or adaptations are made.



STABILITY AND VIBRATIONS OF MICRO-NONHOMOGENEOUS PLATE BAND RESTING ON ELASTIC SUBSOIL

MAREK CHALECKI¹, GRZEGORZ JEMIELITA²

The paper presents a procedure of calculation of natural frequencies and critical buckling forces of a micro-nonhomogeneous plate band resting on nonhomogeneous elastic subsoil and having any given boundary conditions. The band consists of N parts – cells – called elements, having a constant width $l = L/N$. Each band element consists of three parts – subelements with variable widths. The two of these subelements are matrix, the third – inclusion placed symmetrically relative to the matrix. Each band element is built of two isotropic materials. The matrix and inclusion bands have the stiffness and mass per area unit as well as they rest on the subsoil. The model has been derived with use of the classical displacement method. The stiffness matrix of any band element and then the band stiffness matrix have been built. An appropriate computer program has been written to calculate natural frequencies and critical buckling forces. A number of tests have been performed to check the working of the program and several calculative examples has been presented in the paper.

Keywords: natural frequency; buckling; elastic subsoil; displacement method

¹ PhD., Eng., Faculty of Civil and Environmental Engineering, Warsaw University of Life Sciences, Nowoursynowska 166, Warsaw, 02-787, Poland, e-mail: marek_chalecki@sggw.edu.pl

² Prof. Em., PhD., Eng., Faculty of Civil Engineering, Warsaw University of Technology, Armii Ludowej 16, Warsaw, 00-637, Poland, e-mail:

1. INTRODUCTION

Plate bands are very common type of construction. They can serve to model e.g. bridge spans or road surfaces. This latter concerns especially plate bands resting on a subsoil. In the paper, plate band bending to circular surface has been considered. The calculation model used for this purpose is also highly suitable for analysis of bars with variable cross section, resting on elastic subsoil. Thus, the goal of the paper is a presentation of a certain way of calculation of plate bands subjected to the bending to circular surface and resting on elastic subsoil. The band and the subsoil show a functional variability of material properties – here linear (though, assumption of other type of variability is also possible). Such variability model can serve to approximate properties of a transition area between two band-subsoil systems with properties changing along the band width, e.g. a road. Due to the applied modelling algorithm which imposes assumption of periodic properties, it has been assumed that the position of inhomogeneities (e.g. inclusions) of the band strictly corresponds to the position of inhomogeneities of the subsoil. However, it allows assumption of a homogeneous band on a non-homogeneous subsoil or vice-versa. Such way of solving can be applied to perpendicular plates as well. The paper considers a model of micro-nonhomogeneous (functionally graded material, FGM) plate band with the functional heterogeneity of material features along the direction of action of large axial forces (it has been assumed that this is the direction of x -axis). The plate rests on nonhomogeneous elastic subsoil (Fig. 1). In the second direction (y) the band is homogeneous. It has been assumed that the band stiffness does not depend on the y variable. The model includes free vibrations and buckling of the band as well as the subsoil elasticity. For such problem it is possible to obtain an exact (or formally exact) solution within the framework of the theory of thin plates. If the bending elasticity and density of the band, the subsoil stiffness as well as boundary conditions do not depend on the y variable and there is no forces exciting vibrations, the differential equation of plate vibrations can be presented in the form

$$(1.1) \quad D \frac{\partial^4 \widehat{w}(x, t)}{\partial x^4} + S \frac{\partial^2 \widehat{w}(x, t)}{\partial x^2} + \mu \frac{\partial^2 \widehat{w}(x, t)}{\partial t^2} + k \widehat{w}(x, t) = 0$$

where the denotations are assumed: S – band compressing force $\left[\frac{N}{m} \right]$, $D = \frac{E(x)h^3}{12(1-\nu^2(x))}$ – band stiffness $[Nm]$, $\mu = \mu(x)$ – mass per area unit $\left[\frac{kg}{m^2} \right]$, $k = k(x)$ – subsoil stiffness $\left[\frac{N}{m^3} \right]$.

If the harmonic vibrations $\widehat{w}(x, t) = w(x)\cos(\omega t)$ are being considered, the differential equation for amplitudes $w(x)$ is written as follows:

$$(1.2) \quad \frac{d^4 w(\xi)}{d\xi^4} + 2\sigma^2 \frac{d^2 w(\xi)}{d\xi^2} - \lambda^4 w(\xi) = 0$$

$$\sigma^2 = \frac{S\rho}{2D}, \lambda^4 = \lambda_D^4 - \lambda_K^4, \lambda_D^4 = \frac{\mu l^4 \omega^2}{D}, \lambda_K^4 = \frac{kl^4}{D}$$

where ω – vibration angular frequency $\left[\frac{1}{s}\right]$, $\xi = \frac{x}{l}$.

The Eq. (1.1) is identical with the equation of vibrations of longitudinally compressed beam with the unit width and a height h , resting on nonhomogeneous elastic subsoil.

In the case of FGM materials (and periodically varying ones as well), large oscillations (jump-type variability) of the band stiffness make Eq. (1.1) very hard to solve by means of classical methods of mathematics. This problem is usually overcome by application of various techniques of homogenization.

In the literature, generally, one can easily find works concerning statics, stability or vibrations of bars and plates resting on elastic subsoil, but treating these problems separately. However, the case of vibrations of a compressed (buckled) plate (plate band, bar) resting on elastic subsoil, additionally with assumption of variability of material properties of the plate and subsoil, has been much less investigated. Kączkowski [1] analysed statics and stability of rectangular plates and plate bands resting on the Winkler subsoil. In the case of the statics and stability of beams on elastic subsoil, we obtain ordinary differential equations which can be solved with use of classical methods, including Fourier series [2 ÷ 4]. The same applies to the plates [2, 5 ÷ 8] where approximating methods (Ritz [9] or FEM [10]) can be used as well. In the case of the problem being analysed in this work, i.e. stability and vibrations of micro-nonhomogeneous plate band resting on elastic subsoil, an exact solution was obtained in [5] for the stability and in [6] for the vibrations. Many approximated solutions for micro-nonhomogeneous bands resting on homogeneous or non-homogeneous elastic subsoil were obtained with use of the tolerance averaging technique or method of microlocal parameters [11 ÷ 21]. Calculation of equivalent modules is also commonly used – with application of the method of microlocal parameters [22] or homogenization [23 ÷ 25].

Wierzbicki et al. [12] stated as follows: “From among many known ways of the modeling of problems of the mechanics of periodic media, the tolerance modeling stands out due to relative simplicity of consideration of the scale effect. This advantage of the tolerance modeling resulted in the description and solution of many problems of the mechanics of heterogeneous media. Unfortunately, only approximate solutions can be obtained here and effective methods of evaluation of the accuracy of the obtained solutions are not known”. Disagreeing with this statement, the Authors decided to prove

that in the case of the problems presented in [11, 13 ÷ 16], solution can be obtained which is exact [5, 6] or formally exact [2] within the framework of the theory of thin plates.

The FGM plates under consideration have been modeled as a system with features varying in a discrete way. For such a model of the FGM plate band (i.e. having infinite length along the y axis) with the microstructure presented in Fig. 1, this paper presents the possibility to obtain an exact solution of the problem of seeking of natural frequencies and buckling critical force with taking the subsoil elasticity into account. According to the authors' knowledge, there are no items in the literature where the mentioned problem would be solved in such way.

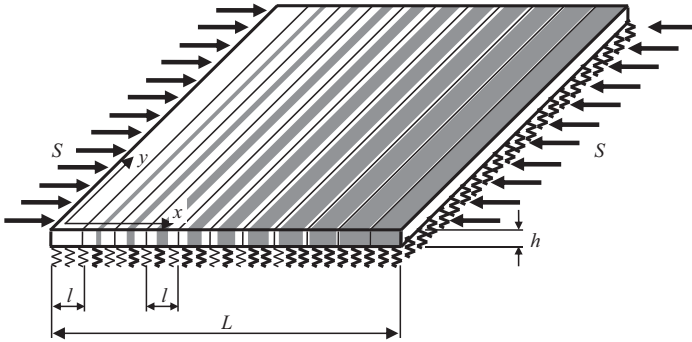


Fig. 1. Plate band having a microstructure and resting on elastic subsoil

2. BASIC ASSUMPTIONS

Let us consider a Kirchhoff plate band having a length L and thickness h as well as the microstructure presented in Fig. 1. Along the x variable, the band consists of N bands – cells, further referred to as elements – of a constant length $l = L/N$. Each element consists of three parts (subelements) and two isotropic materials: 1 (matrix) and 2 (inclusion). It has been assumed that in each element the inclusion is placed symmetrically relative to the matrix. The element is characterized by following quantities: matrix and inclusion stiffnesses D_1, D_2 , masses per area unit μ_1, μ_2 , subsoil stiffnesses k_1, k_2 (Fig. 2), wherein

$$D_1 = D = \frac{E_1 h^3}{12(1-\nu_1^2)} = \frac{E h^3}{12(1-\nu^2)}, \quad D_2 = \delta D, \quad D > 0,$$

$$\mu_1 = \mu = \rho h, \quad \mu_2 = r\mu, \quad \mu > 0, \quad k_1 = k, \quad k_2 = \kappa k.$$

where δ – any real number greater than 0, r, κ – any real numbers greater than or equal to 0.

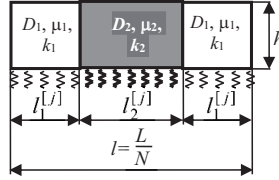


Fig. 2. Dimensions of a cell

The lengths of the subelements of the j -th element are calculated from the formulas

$$l_1^{[j]} = \xi_1^{[j]} l^{[j]}, \quad l_2^{[j]} = \xi_2^{[j]} l^{[j]},$$

where the fraction coefficients ξ_1, ξ_2 and the cell length l are calculated as

$$(2.1) \quad \xi_1^{[j]} = \frac{1}{2} \left(1 - \frac{j-1}{N-1} \right), \quad \xi_2^{[j]} = \frac{j-1}{N-1}, \quad j = 1, 2, 3, \dots, N, \quad l^{[j]} = 2l_1^{[j]} + l_2^{[j]} = \frac{L}{N}.$$

The solution of the Eq. (1.2), depending on the subelement, is written in a form

$$(2.2) \quad w(\xi) = C_1 \text{ch}(\eta\xi) + C_2 \text{sh}(\eta\xi) + C_3 \text{ch}(\tau\xi) + C_4 \text{sh}(\tau\xi),$$

wherein, after introduction of local systems of coordinates

$$(2.3) \quad \xi = \frac{x}{l^{[j]}}, \quad 0 \leq \xi \leq 1, \quad \eta_k = \sqrt{\sigma_k^4 + \lambda_k^4 - \sigma_k^2}, \quad \tau_k = \sqrt{\sigma_k^4 + \lambda_k^4 + \sigma_k^2},$$

$$\sigma_k^2 = \frac{S}{2D_k} \left(l^{[j]} \right)^2, \quad \lambda_k^4 = \frac{\left(l^{[j]} \right)^4}{D_k} (\mu_k \omega^2 - k_k),$$

and the subscript $k = 1$ concerns the matrix subelement, $k = 2$ – the inclusion subelement.

3. TRANSFORMATION FORMULAS OF A BAND ELEMENT

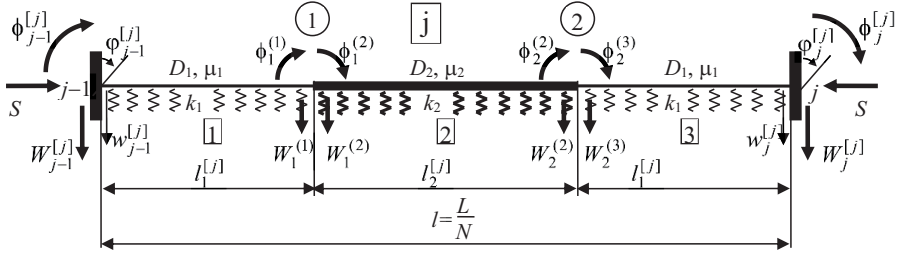


Fig. 3. Model of the band element having a number $[j]$

Fig. 3 presents a one-dimensional scheme of a band element which can be treated as a bar, clamped on both edges, having a consecutive number j , length $l = L/N$, jump-type variable stiffness as well as mass per area unit and resting on a subsoil with jump-type variable elasticity. It has been assumed that the external nodes $(j - 1)$ and (j) of this bar are subjected to displacements (rotations and relocations) with amplitudes $\phi_{j-1}^{[j]}, \phi_j^{[j]}, w_{j-1}^{[j]}, w_j^{[j]}$ (Fig.3). Using the formulas (2.2) and (2.3), considering boundary conditions, the dependences between node forces and node displacements for the subelements can be determined and written in a form:

$$(3.1) \quad \Phi_i = \mathbf{K}_i \mathbf{q}_i, \quad i = 1, 2, 3,$$

where \mathbf{K}_i is a stiffness matrix of an i -th subelement and

$$\Phi_1 = \begin{bmatrix} \Phi_{(j-1)}^{[j]} \\ \Phi_{(1)}^{[j]} \\ W_{(j-1)}^{[j]} l_1^{[j]} \\ W_{(1)}^{[j]} l_1^{[j]} \end{bmatrix}, \quad \Phi_2 = \begin{bmatrix} \Phi_{(1)}^{[j]} \\ \Phi_{(2)}^{[j]} \\ W_{(1)}^{[j]} l_2^{[j]} \\ W_{(2)}^{[j]} l_2^{[j]} \end{bmatrix}, \quad \Phi_3 = \begin{bmatrix} \Phi_{(2)}^{[j]} \\ \Phi_{(j)}^{[j]} \\ W_{(2)}^{[j]} l_1^{[j]} \\ W_{(j)}^{[j]} l_1^{[j]} \end{bmatrix}, \quad \mathbf{q}_1 = \begin{bmatrix} \phi_{(j-1)}^{[j]} \\ \phi_{(1)}^{[j]} \\ \psi_{(j-1)}^{[j]} \\ \frac{\psi_{(1)}^{[j]}}{\xi_1^{[j]}} \\ \psi_{(1)}^{[j]} \\ \frac{\psi_{(2)}^{[j]}}{\xi_1^{[j]}} \end{bmatrix}, \quad \mathbf{q}_2 = \begin{bmatrix} \phi_{(1)}^{[j]} \\ \phi_{(2)}^{[j]} \\ \psi_{(1)}^{[j]} \\ \frac{\psi_{(2)}^{[j]}}{\xi_2^{[j]}} \\ \psi_{(2)}^{[j]} \\ \frac{\psi_{(j)}^{[j]}}{\xi_2^{[j]}} \end{bmatrix}, \quad \mathbf{q}_3 = \begin{bmatrix} \phi_{(2)}^{[j]} \\ \phi_{(j)}^{[j]} \\ \psi_{(2)}^{[j]} \\ \frac{\psi_{(j)}^{[j]}}{\xi_1^{[j]}} \\ \psi_{(j)}^{[j]} \\ \frac{\psi_{(j)}^{[j]}}{\xi_1^{[j]}} \end{bmatrix},$$

$$\mathbf{K}_1 = \mathbf{K}_3 = \frac{D_1}{l_1^{[j]}} \begin{bmatrix} \alpha_1^{[j]} & \beta_1^{[j]} & \theta_1^{[j]} & -\delta_1^{[j]} \\ \beta_1^{[j]} & \alpha_1^{[j]} & \delta_1^{[j]} & -\theta_1^{[j]} \\ \theta_1^{[j]} & \delta_1^{[j]} & \gamma_1^{[j]} & -\varepsilon_1^{[j]} \\ -\delta_1^{[j]} & -\theta_1^{[j]} & -\varepsilon_1^{[j]} & \gamma_1^{[j]} \end{bmatrix}, \quad \mathbf{K}_2 = \frac{D_2}{l_2^{[j]}} \begin{bmatrix} \alpha_2^{[j]} & \beta_2^{[j]} & \theta_2^{[j]} & -\delta_2^{[j]} \\ \beta_2^{[j]} & \alpha_2^{[j]} & \delta_2^{[j]} & -\theta_2^{[j]} \\ \theta_2^{[j]} & \delta_2^{[j]} & \gamma_2^{[j]} & -\varepsilon_2^{[j]} \\ -\delta_2^{[j]} & -\theta_2^{[j]} & -\varepsilon_2^{[j]} & \gamma_2^{[j]} \end{bmatrix},$$

$$\begin{aligned}
 \Psi_{(j-1)}^{[j]} &= \frac{w_{(j-1)}^{[j]}}{l}, \quad \Psi_{(1)}^{[j]} = \frac{w_{(1)}^{[j]}}{l}, \quad \Psi_{(2)}^{[j]} = \frac{w_{(2)}^{[j]}}{l}, \quad \Psi_{(j)}^{[j]} = \frac{w_{(j)}^{[j]}}{l}, \\
 (3.2) \quad \alpha_k &= \frac{(\eta_k^2 + \tau_k^2)(\eta_k \operatorname{ch} \eta_k \sin \eta_k - \tau_k \cos \eta_k \operatorname{sh} \eta_k)}{\Delta_k}, \quad \beta_k = \frac{(\eta_k^2 + \tau_k^2)(\tau_k \operatorname{sh} \eta_k - \eta_k \sin \tau_k)}{\Delta_k}, \\
 \theta_k &= \frac{\eta_k \tau_k ((\tau_k^2 - \eta_k^2)(1 - \operatorname{ch} \eta_k \cos \tau_k) + 2\eta_k \tau_k \operatorname{sh} \eta_k \sin \tau_k)}{\Delta_k}, \quad \delta_k = \frac{\eta_k \tau_k (\eta_k^2 + \tau_k^2)(\operatorname{ch} \eta_k - \cos \tau_k)}{\Delta_k}, \\
 \gamma_k &= \frac{\eta_k \tau_k (\eta_k^2 + \tau_k^2)(\tau_k \operatorname{ch} \eta_k \sin \tau_k + \eta_k \operatorname{sh} \eta_k \cos \tau_k)}{\Delta_k}, \quad \varepsilon_k = \frac{\eta_k \tau_k (\eta_k^2 + \tau_k^2)(\tau_k \sin \tau_k + \eta_k \operatorname{sh} \eta_k)}{\Delta_k}, \\
 \Delta_k &= 2\eta_k \tau_k - 2\eta_k \tau_k \operatorname{ch} \eta_k \cos \eta_k + (\eta_k^2 - \tau_k^2) \operatorname{sh} \eta_k \sin \eta_k, \quad k = 1, 2.
 \end{aligned}$$

It must be emphasized that Forms. (3.2) concern any homogeneous vibrating band subelement having both endings clamped, being subjected to the acting of a big axial force, resting on elastic subsoil for which the coefficients η_k and τ_k are described by Form. (2.3).

4. ELEMENT (CELL) STIFFNESS MATRIX

The dependence of the node moments $\phi_{(j-1)}^{[j]}$, $\phi_{(j)}^{[j]}$ and forces $W_{(j-1)}^{[j]}$, $W_{(j)}^{[j]}$ on the displacements $\varphi_{(j-1)}^{[j]}$, $\varphi_{(j)}^{[j]}$, $\Psi_{(j-1)}^{[j]}$, $\Psi_{(j)}^{[j]}$ of the band element can be written in a form

$$(4.1) \quad \Phi^{[j]} = \mathbf{K}^{[j]} \varphi^{[j]}$$

where $\mathbf{K}^{[j]}$ is a band element stiffness matrix and

$$\Phi^{[j]} = \begin{bmatrix} \phi_{(j-1)}^{[j]} \\ \phi_{(j)}^{[j]} \\ W_{(j-1)}^{[j]} \\ W_{(j)}^{[j]} \end{bmatrix}, \quad \varphi^{[j]} = \begin{bmatrix} \varphi_{(j-1)}^{[j]} \\ \varphi_{(j)}^{[j]} \\ 2\Psi_{(j-1)}^{[j]} \\ 2\Psi_{(j)}^{[j]} \end{bmatrix}.$$

Application of the condition of equilibrium in the nodes (1) i (2)

$$\phi_{(1)}^{[1]} + \phi_{(1)}^{[2]} = 0, \quad \phi_{(2)}^{[2]} + \phi_{(2)}^{[3]} = 0, \quad W_{(1)}^{[1]} + W_{(1)}^{[2]} = 0, \quad W_{(2)}^{[2]} + W_{(2)}^{[3]} = 0,$$

yields in the following set of equations

$$(4.2) \quad \mathbf{R}^{[j]} \mathbf{f}^{[j]} + \mathbf{R}_0^{[j]} \mathbf{f}_0^{[j]} = 0,$$

where

$$\mathbf{R}^{[j]} = \begin{bmatrix} r_{11} & r_{12} & r_{13} & r_{14} \\ r_{12} & r_{11} & -r_{14} & -r_{13} \\ r_{13} & -r_{14} & r_{33} & r_{34} \\ r_{14} & -r_{13} & r_{34} & r_{33} \end{bmatrix}, \mathbf{R}_0^{[j]} = \begin{bmatrix} r_{011} & 0 & r_{013} & 0 \\ 0 & r_{011} & 0 & -r_{013} \\ -r_{013} & 0 & r_{033} & 0 \\ 0 & r_{013} & 0 & r_{033} \end{bmatrix}, \mathbf{f}^{[j]} = \begin{bmatrix} \varphi_{(1)}^{[j]} \\ \varphi_{(2)}^{[j]} \\ \psi_{(1)}^{[j]} \\ \psi_{(2)}^{[j]} \end{bmatrix}, \mathbf{f}_0^{[j]} = \begin{bmatrix} \varphi_{(j-1)}^{[j]} \\ \varphi_{(j)}^{[j]} \\ \psi_{(j-1)}^{[j]} \\ \psi_{(j)}^{[j]} \end{bmatrix}$$

$$r_{11} = \frac{\alpha_1^{[j]}}{\xi_1^{[j]}} + \frac{\eta \alpha_2^{[j]}}{\xi_2^{[j]}}, \quad r_{011} = \frac{\beta_1^{[j]}}{\xi_1^{[j]}}, \quad r_{12} = \frac{\eta \beta_2^{[j]}}{\xi_2^{[j]}}, \quad r_{13} = \frac{\eta \theta_2^{[j]}}{(\xi_2^{[j]})^2} - \frac{\theta_1^{[j]}}{(\xi_1^{[j]})^2}, \quad r_{013} = \frac{\delta_1^{[j]}}{(\xi_1^{[j]})^2},$$

$$r_{14} = -\frac{\eta \delta_2^{[j]}}{(\xi_2^{[j]})^2}, \quad r_{33} = \frac{\gamma_1^{[j]}}{(\xi_1^{[j]})^3} + \frac{\eta \gamma_2^{[j]}}{(\xi_2^{[j]})^3}, \quad r_{033} = -\frac{\varepsilon_1^{[j]}}{(\xi_1^{[j]})^3}, \quad r_{34} = -\frac{\eta \varepsilon_2^{[j]}}{(\xi_2^{[j]})^3}.$$

The solution of the set (4.2) are the displacements $\varphi_1^{[j]}, \varphi_2^{[j]}, \psi_1^{[j]}, \psi_2^{[j]}$, depending on the displacements in the nodes $(j-1)$ and (j) , i.e. on $\varphi_{j-1}^{[j]}, \varphi_j^{[j]}, \psi_{j-1}^{[j]}, \psi_j^{[j]}$, in the following way:

$$(4.3) \quad \begin{aligned} \varphi_{(1)}^{[j]} &= A_1^{[j]} \varphi_{(j-1)}^{[j]} + B_1^{[j]} \psi_{(j-1)}^{[j]} + C_1^{[j]} \varphi_{(j)}^{[j]} - D_1^{[j]} \psi_{(j)}^{[j]}, \\ \varphi_{(2)}^{[j]} &= C_1^{[j]} \varphi_{(j-1)}^{[j]} + D_1^{[j]} \psi_{(j-1)}^{[j]} + A_1^{[j]} \varphi_{(j)}^{[j]} - B_1^{[j]} \psi_{(j)}^{[j]}, \\ \psi_{(1)}^{[j]} &= A_2^{[j]} \varphi_{(j-1)}^{[j]} + B_2^{[j]} \psi_{(j-1)}^{[j]} + C_2^{[j]} \varphi_{(j)}^{[j]} - D_2^{[j]} \psi_{(j)}^{[j]}, \\ \psi_{(2)}^{[j]} &= -C_2^{[j]} \varphi_{(j-1)}^{[j]} - D_2^{[j]} \psi_{(j-1)}^{[j]} - A_2^{[j]} \varphi_{(j)}^{[j]} + B_2^{[j]} \psi_{(j)}^{[j]}, \end{aligned}$$

where in the coefficients $A_1 \dots D_2$ are the terms of the matrix $(-\mathbf{R}^{[j]})^{-1} \mathbf{R}_0^{[j]}$ for the given j -th element (cell). The algebraic form of these coefficients is spacious (each of them occupies ca. one A4 page), so the corresponding formulas are omitted in this paper.

Using (3.1), for $i=1$ and $i=3$ one obtains the following dependences connecting moments and forces in the external nodes $(j-1)$ and (j) to the displacements in these external nodes $\varphi_{(j-1)}^{[j]}, \psi_{(j-1)}^{[j]}, \varphi_{(j)}^{[j]}, \psi_{(j)}^{[j]}$ and in the internal ones $\varphi_{(1)}^{[j]}, \psi_{(1)}^{[j]}, \varphi_{(2)}^{[j]}, \psi_{(2)}^{[j]}$:

$$\begin{aligned}
 (4.4) \quad \Phi_{(j-1)}^{[j]} &= \frac{D}{\xi_1^{[j]l}} \left[\alpha_1^{[j]} \Phi_{(j-1)}^{[j]} + \beta_1^{[j]} \Phi_{(1)}^{[j]} + \theta_1^{[j]} \frac{\Psi_{(j-1)}^{[j]}}{\xi_1^{[j]}} - \delta_1^{[j]} \frac{\Psi_{(1)}^{[j]}}{\xi_1^{[j]}} \right], \\
 \Phi_{(j)}^{[j]} &= \frac{D}{\xi_2^{[j]l}} \left[\beta_1^{[j]} \Phi_{(2)}^{[j]} + \alpha_1^{[j]} \Phi_{(j)}^{[j]} + \delta_1^{[j]} \frac{\Psi_{(2)}^{[j]}}{\xi_1^{[j]}} - \theta_1^{[j]} \frac{\Psi_{(j)}^{[j]}}{\xi_1^{[j]}} \right], \\
 W_{(j-1)}^{[j]} &= \frac{D}{(\xi_1^{[j]l})^2} \left[\theta_1^{[j]} \Phi_{(j-1)}^{[j]} + \delta_1^{[j]} \Phi_{(1)}^{[j]} + \gamma_1^{[j]} \frac{\Psi_{(j-1)}^{[j]}}{\xi_1^{[j]}} - \varepsilon_1^{[j]} \frac{\Psi_{(1)}^{[j]}}{\xi_1^{[j]}} \right], \\
 W_{(j)}^{[j]} &= -\frac{D}{(\xi_1^{[j]l})^2} \left[\delta_1^{[j]} \Phi_{(2)}^{[j]} + \theta_1^{[j]} \Phi_{(j)}^{[j]} + \varepsilon_1^{[j]} \frac{\Psi_{(2)}^{[j]}}{\xi_1^{[j]}} - \gamma_1^{[j]} \frac{\Psi_{(j)}^{[j]}}{\xi_1^{[j]}} \right].
 \end{aligned}$$

Special attention must be paid to the first and last element, i.e. for $j = 1$ and $j = N$. The terms ξ_1 and ξ_2 take here the values (cf. Eq. 2.1): $\xi_1^{[1]} = \frac{1}{2N}$ and $\xi_2^{[1]} = 0$ for $j = 1$, $\xi_1^{[N]} = 0$ and $\xi_2^{[N]} = \frac{1}{N}$ for $j = N$. The first cell has the constant stiffness D , whereas the last one – the constant stiffness $D_2 = \eta D$. Moreover, generally these cells are not supported as in Fig. 3 because the left support of the first cell as well as the right support of the last cell are identical to the real supports of the band. The transformation formulas for the first and last cells are derived in accordance with the band supports in analogical way as for the bar with both endings clamped.

After the substitution of the determined displacements $\Phi_{(1)}^{[j]}, \Phi_{(2)}^{[j]}, \Psi_{(1)}^{[j]}, \Psi_{(2)}^{[j]}$ (form. 4.3) to the formulas (4.4), these latter have been written in a form of Eq. (4.1), where the stiffness matrix $\mathbf{K}^{[j]}$ of the j -th element of the band has a form

$$\mathbf{K}^{[j]} = \begin{bmatrix} k_{11} & k_{12} & k_{13} & k_{14} \\ k_{12} & k_{11} & -k_{14} & -k_{13} \\ k_{13} & -k_{14} & k_{33} & k_{34} \\ k_{14} & -k_{13} & k_{34} & k_{33} \end{bmatrix}.$$

The individual terms k are equal:

$$\begin{aligned}
 (4.5) \quad k_{11} &= \frac{c_1^{[j]} \beta_1^{[j]}}{2\xi_1^{[j]}} - \frac{c_2^{[j]} \delta_1^{[j]}}{2(\xi_1^{[j]})^2}, \quad k_{12} = \frac{A_1^{[j]} \beta_1^{[j]}}{2\xi_1^{[j]}} + \frac{\alpha_1^{[j]}}{2\xi_1^{[j]}} - \frac{A_2^{[j]} \delta_1^{[j]}}{2(\xi_1^{[j]})^2}, \quad k_{13} = \frac{D_1^{[j]} \beta_1^{[j]}}{4\xi_1^{[j]}} - \frac{D_2^{[j]} \delta_1^{[j]}}{(2\xi_1^{[j]})^2}, \\
 k_{14} &= -\frac{B_1^{[j]} \beta_1^{[j]}}{4\xi_1^{[j]}} - \frac{\theta_1^{[j]}}{(2\xi_1^{[j]})^2} + B_2^{[j]} \delta_1^{[j]} \frac{1}{(2\xi_1^{[j]})^2}, \quad k_{33} = -\frac{D_1^{[j]} \delta_1^{[j]}}{2(2\xi_1^{[j]})^2} + \frac{D_2^{[j]} \varepsilon_1^{[j]}}{(2\xi_1^{[j]})^2}, \\
 k_{34} &= -\frac{B_1^{[j]} \delta_1^{[j]}}{2(2\xi_1^{[j]})^2} + \frac{\gamma_1^{[j]}}{(2\xi_1^{[j]})^3} - B_2^{[j]} \varepsilon_1^{[j]} \frac{1}{(2\xi_1^{[j]})^3}.
 \end{aligned}$$

The structure of the matrices \mathbf{K} and $\boldsymbol{\varphi}$ is presented in the Eq. 5.1 (the empty cells are equal 0). The matrix \mathbf{K} is divided into pairs of rows. The individual terms are equal:

$$\begin{aligned} a^{(i)} &= k_{12}^{(i)} + k_{12}^{(i+1)}, \quad a' = \frac{1}{2}\alpha_p + k_{12}^{(2)}, \quad a'' = \frac{1}{2}\eta\alpha_k + k_{12}^{(N-1)}, \quad b^{(i)} = k_{11}^{(i)}, \\ c^{(i)} &= k_{14}^{(i)} + k_{14}^{(i+1)}, \quad c' = -\frac{1}{4}\theta_p + k_{14}^{(2)}, \quad c'' = \frac{1}{4}\eta\theta_k + k_{14}^{(N-1)}, \quad d_1^{(i)} = -k_{13}^{(i)}, \quad d_2^{(i)} = k_{13}^{(i+1)}, \\ g^{(i)} &= k_{34}^{(i)} + k_{34}^{(i+1)}, \quad g' = \frac{1}{8}\gamma_p + k_{34}^{(2)}, \quad g'' = \frac{1}{8}\eta\gamma_k + k_{34}^{(N-1)}, \quad h^{(i)} = k_{13}^{(i)}, \end{aligned}$$

where the superscript in the terms a, b, c, d, g, h denotes the row pair number, whereas in the terms with the core letter k – the band element (cell) number. Thus, if one calculates e.g. the term g from the 3rd row pair of the matrix \mathbf{K} , it requires to take the component k_{34} for the cell 3; the term d_1 from the 3rd row pair requires to take the component k_{13} for the cell 3, whereas the term d_2 in the same row pair – the term k_{13} for the cell 4. The terms with the core letter k are given by Forms. (4.5).

The terms $a', a'', c', c'', g', g''$ concern the first and the last cell and are the consequence of the fact that the left support of the first cell as well as the right support of the last cell are the same as the real supports of the band. Depending on the type of the supports, the coefficients $\alpha_b, \theta_b, \gamma_b$ and $\alpha_e, \theta_e, \gamma_e$ are equal to:

– for the clamped edge:

$$\alpha_{b/e} = \alpha_{1/2}, \quad \theta_{b/e} = \theta_{1/2}, \quad \gamma_{b/e} = \gamma_{1/2};$$

– for the hinged edge:

$$\begin{aligned} \alpha_{b/e} &= \frac{(\eta_{1/2}^2 + \tau_{1/2}^2) \sin \tau_{1/2} \operatorname{sh} \eta_{1/2}}{\Delta'}, \quad \theta_{b/e} = \frac{\eta_{1/2} \tau_{1/2} (\tau_{1/2} \operatorname{ch} \eta_{1/2} \sin \tau_{1/2} + \eta_{1/2} \operatorname{sh} \eta_{1/2} \cos \tau_{1/2})}{\Delta'}, \\ \gamma_{b/e} &= \frac{\eta_{1/2} \tau_{1/2} (\eta_{1/2}^2 + \tau_{1/2}^2) \cos \tau_{1/2} \operatorname{ch} \eta_{1/2}}{\Delta'}, \quad \Delta' = \eta_{1/2} \sin \tau_{1/2} \operatorname{ch} \eta_{1/2} - \tau_{1/2} \cos \tau_{1/2} \operatorname{sh} \eta_{1/2}; \end{aligned}$$

– for the clamped edge with the possibility of transverse movement:

$$\begin{aligned} \alpha_{b/e} &= \frac{(\eta_{1/2}^2 + \tau_{1/2}^2) \operatorname{ch} \eta_{1/2} \cos \tau_{1/2}}{\Delta''}, \quad \theta_{b/e} = \frac{\eta_{1/2} \tau_{1/2} (\tau_{1/2} \operatorname{sh} \eta_{1/2} \cos \tau_{1/2} - \eta_{1/2} \operatorname{ch} \eta_{1/2} \sin \tau_{1/2})}{\Delta''}, \\ \gamma_{b/e} &= \frac{\eta_{1/2} \tau_{1/2} (\eta_{1/2}^2 + \tau_{1/2}^2) \sin \tau_{1/2} \operatorname{sh} \eta_{1/2}}{\Delta''}, \quad \Delta'' = \tau_{1/2} \operatorname{ch} \eta_{1/2} \sin \tau_{1/2} + \eta_{1/2} \operatorname{sh} \eta_{1/2} \cos \tau_{1/2}; \end{aligned}$$

– for the free edge:

$$\alpha_{b/e} = \frac{(\eta_{1/2}^2 + \tau_{1/2}^2)(\eta_{1/2}^3 \cos \tau_{1/2} \operatorname{sh} \eta_{1/2} - \tau_{1/2}^3 \operatorname{ch} \eta_{1/2} \sin \tau_{1/2})}{\Delta'''},$$

$$\theta_{b/e} = - \frac{\eta_{1/2} \tau_{1/2} (\eta_{1/2} \tau_{1/2} (\eta_{1/2}^2 - \tau_{1/2}^2) (1 - \operatorname{ch} \eta_{1/2} \cos \tau_{1/2}) + (\eta_{1/2}^4 + \tau_{1/2}^4) \operatorname{sh} \eta_{1/2} \sin b_{1/2}) \tau}{\Delta'''},$$

$$\gamma_{b/e} = - \frac{\eta_{1/2} \tau_{1/2} (\eta_{1/2}^2 + \tau_{1/2}^2) (\eta_{1/2}^3 \operatorname{ch} \eta_{1/2} \sin \tau_{1/2} + \tau_{1/2}^3 \operatorname{sh} \eta_{1/2} \cos \tau_{1/2})}{\Delta'''},$$

$$\Delta''' = (\eta_{1/2}^4 + \tau_{1/2}^4) \operatorname{ch} \eta_{1/2} \cos \tau_{1/2} + \eta_{1/2} \tau_{1/2} (2 \eta_{1/2} \tau_{1/2} (\eta_{1/2}^2 - \tau_{1/2}^2) \operatorname{sh} \eta_{1/2} \sin \tau_{1/2}).$$

The subscripts b and e denote the beginning and end support of the band, respectively. If the beginning edge is being considered in the calculation, one must choose the terms η_1, τ_1 , whereas if the ending one – the terms η_2, τ_2 .

6. CALCULATION OF THE VALUES OF NATURAL FREQUENCY AND CRITICAL BUCKLING FORCE

The natural frequency ω_0 and critical buckling force S_{cr} , which are ultimately being sought, are calculated from the condition $\operatorname{Det} \mathbf{K} = 0$. Both of these quantities are unknowns in the determinant $\operatorname{Det} \mathbf{K}$, hence two procedures are possible:

- 1) Assume consecutive values of axial compressing forces S and calculate the natural frequencies ω_0 from the condition $\operatorname{Det} \mathbf{K} = 0$ for the given parameters of the band and subsoil stiffness. The result is a diagram of the function $\omega(S)$. The points of intersection of the diagram branches with the abscissa denote the static critical buckling force S_{cr} , whereas the points of intersection with the ordinate – the natural frequency ω_0 .
- 2) Assume consecutive values of the frequency of forced vibrations ω and calculate the critical buckling force S_{cr} from the condition $\operatorname{Det} \mathbf{K} = 0$. The result is a diagram of the function $S(\omega)$. The points of intersection of the diagram branches with the ordinate denote the static critical buckling force S_{cr} , whereas the points of intersection with the abscissa – the natural frequency ω_0 .

However, the matrix \mathbf{K} generally has large dimensions, its terms depend on the functions given by Forms. (3.2) in a very complicated way and additionally those functions depend on the values of ω and S . Thus, such functional dependence is extremely intricate and the determination of subsequent zeros can take a lot of time even for computers with good processors. Therefore the best way is to

assume an initial value of S or ω and, for a given step of increase of this initial value, after the determinant value has changed the sign, apply the secant method for finding such a value of S_{cr} or ω_0 which implies $\text{Det}\mathbf{K}(S_{cr}) \cong 0$ or $\text{Det}\mathbf{K}(\omega_0) \cong 0$, respectively. This value can be determined with any required accuracy.

The described procedures are characterized by the same level of complication, so it does not matter which to choose. For the further considerations, the procedure 2 has been chosen.

7. EXAMPLES

7.1. EXAMPLE 1

Let us consider a band having 8 cells ($N = 8$) and both edges clamped. The matrix stiffness equals to $D = 1,333 \cdot 10^5$ kNm, the matrix unit mass $\mu = 4000$ kg/m², the cell length $l = 1$ m. In the first version a homogeneous band without subsoil has been assumed, hence $r = 1$, $\eta = 1$, $k = 0$. The result is the diagram presented in Fig. 5a. Three branches are visible in the assumed range of the frequency of forced vibrations ω and compressing force S – from these branches always the lowest values must be chosen because only the first (the lowest) critical buckling force is essential (has physical meaning). Therefore, only the points on the heavy lines have the practical meaning.

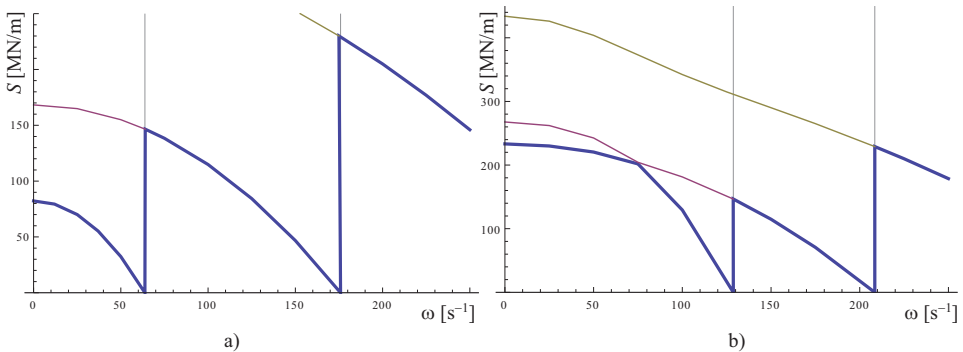


Fig. 5. Diagram $S(\omega)$ for a homogeneous band: a) without subsoil, b) with subsoil

The analysis of the values of static critical buckling force and natural frequencies for zero compressing force proves that these values correspond to those known from the mechanics for a beam with both endings clamped provided the beam stiffness EJ is changed to the plate stiffness D :

$$S_{cr} = \frac{4\pi^2 D}{(N)^2} = 82,24 \text{ MN/m}, \quad \omega_{01} = 4,73^2 \sqrt{\frac{D}{\mu(N)^4}} = 63,82 \text{ s}^{-1}, \quad \omega_{02} = 7,85^2 \sqrt{\frac{D}{\mu(N)^4}} = 175,93 \text{ s}^{-1}.$$

In the **second version** a subsoil with the stiffness $k = 50000 \text{ kN/m}^3$ has been assumed. The band remains homogeneous, thus the subsoil must be assumed as homogeneous ($\kappa = 1$). The result is a diagram presented in Fig. 5b. One can see that the branches can cross with each other what is due the fact that the determinant $\text{Det}\mathbf{K}(S, \omega)$ can have double zeros for this case.

In the **third version** a heterogeneous subsoil with the heterogeneity coefficients $r = 2, \delta = 2, \kappa = 2$ has been assumed (the stiffness k – as in the version 2). The result is a diagram presented in Fig. 6a. One can see that the diagram branches do not cross with each other, although they demonstrate such trend. The fact that the branches do not cross with each other can be proved if the density of points around the alleged intersection point is increased – there will be no common point for two branches what shows that the determinant $\text{Det}\mathbf{K}(S, \omega)$ for such bands does not have double zeros. The tendency of approaching of the branches to each other is the stronger the more cells is in the band (Fig. 6b).

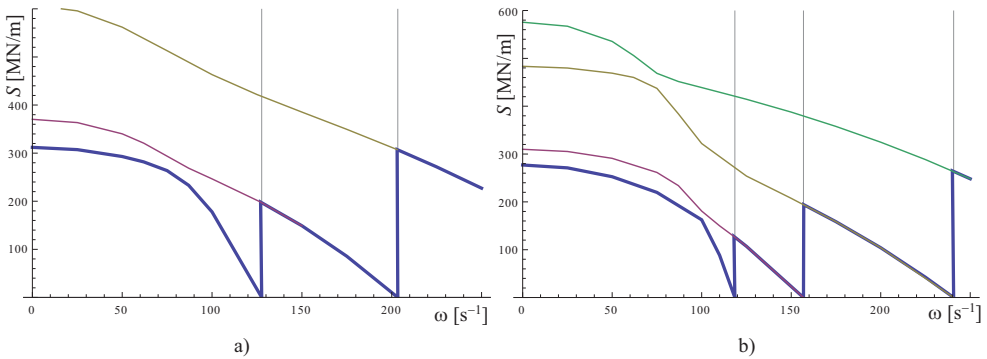


Fig. 6. Diagram $S(\omega)$ for the heterogeneous band with subsoil: a) $N = 8$, b) $N = 10$

7.2. EXAMPLE 2

As for homogeneous beams not resting on a subsoil the values of critical buckling forces and natural frequencies are known, it has been investigated what values of ω_0 and S_{cr} would be obtained for homogeneous bands without subsoil, calculated with the procedure being presented in the paper. It can be acknowledged as a kind of a correctness test of this procedure. The result for the band with both edges clamped (with 8 cells) has been already presented in Fig. 5.

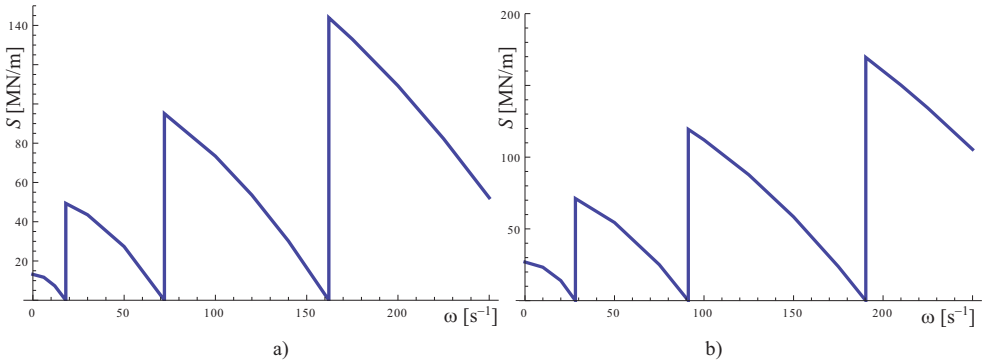


Fig. 7. Diagram $S(\omega)$ for the homogeneous band without subsoil: a) with both edges hinged, b) with the one edge clamped and the other hinged

Fig. 7 presents the diagrams for 10-cell bands (D, μ, l – as in Example 1) from which the one has both edges hinged (a) and the second – the one edge clamped and the other hinged (b). It has been obtained:

– for the band „a”: $S_{cr} = \frac{\pi^2 D}{(N)^2} = 13,60 \text{ MN/m}$, $\omega_{01} = \pi^2 \sqrt{\frac{D}{\mu(N)^4}} = 18,02 \text{ s}^{-1}$,

$$\omega_{02} = (2\pi)^2 \sqrt{\frac{D}{\mu(N)^4}} = 72,08 \text{ s}^{-1}, \quad \omega_{03} = (3\pi)^2 \sqrt{\frac{D}{\mu(N)^4}} = 162,17 \text{ s}^{-1};$$

– for the band „b”: $S_{cr} = \frac{\pi^2 D}{(0,699N)^2} = 26,92 \text{ MN/m}$, $\omega_{01} = 3,927^2 \sqrt{\frac{D}{\mu(N)^4}} = 28,15 \text{ s}^{-1}$,

$$\omega_{02} = 7,069^2 \sqrt{\frac{D}{\mu(N)^4}} = 91,23 \text{ s}^{-1}, \quad \omega_{03} = 10,21^2 \sqrt{\frac{D}{\mu(N)^4}} = 190,32 \text{ s}^{-1}.$$

The obtained results comply with those known from the theory.

7.3. EXAMPLE 3

If for several bands with the same length the total amount of inclusion varies linearly along with the coordinate x , according to Form. (2.1), then such bands should be characterized by the same values of critical buckling forces and natural frequencies, regardless of the fact into how many cells they have been divided. To check how the procedure operates in this regard, four heterogeneous bands have been considered, having the parameters D, k, μ such as in Example 1, the total length $L = 10 \text{ m}$ and divided consecutively into 4, 6, 8 and 10 cells (i.e. the cell length l is equal: 2.5 m, $\frac{5}{3} \text{ m}$, 1.25 m and 1 m, respectively). The result is the diagram in Fig. 8. One can see that the lines practically cover each other – the inaccuracies are the higher the lower is the cell number N . It proves that the procedure

describes the behavior of the bands with the same length and the same amount of inclusions in the same way, regardless of the cell number N .

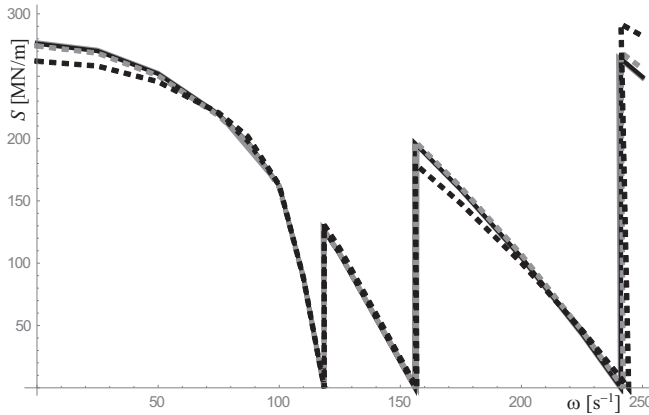


Fig. 8. Diagram $S(\omega)$ for the heterogeneous bands having the same length:

..... $N = 4$, $N = 6$, — $N = 8$, — $N = 10$

7.4. EXAMPLE 4

The results for four bands (Fig. 9) have been compared: two of them have both edges clamped, two other – the one edge clamped and the other hinged. The bands from each pair are identical but the one is oriented in opposite direction in comparison to the other. The first band of each pair (in Fig. 9 – the upper one) has the parameters: $D = 1.333 \cdot 10^5$ kNm, $\mu = 4000$ kg/m, $k = 50000$ kN/m³, $l = 1$ m, $N = 6$, $\delta = 2$, $r = 2$, $\kappa = 2$, i.e. it starts in the left edge with the cell having a lower stiffness and finishes in the right edge with the cell having a higher stiffness. On account of that the second band from each pair (in Fig. 9 – the lower one) – as it is identical to the first but oriented in the opposite direction – has the parameters: $D = 2.667 \cdot 10^5$ kNm, $\mu = 8000$ kg/m, $k = 100000$ kN/m³, $l = 1$ m, $N = 6$, $\delta = 0.5$, $r = 0.5$, $\kappa = 0.5$.

It results from Fig. 9 that the procedure is not sensitive to the inversion of the cell sequence – the results for each pair cover with each other. The condition is that the reference material parameters (concerning the cell 1 – D , μ , k) for the band with the inversed cell sequence must be δ , r , κ times greater than for the band with the original sequence, whereas the heterogeneity coefficients (δ , r , κ) for the band with the inversed cell sequence must be the inverse of the coefficients for the band with the original sequence.

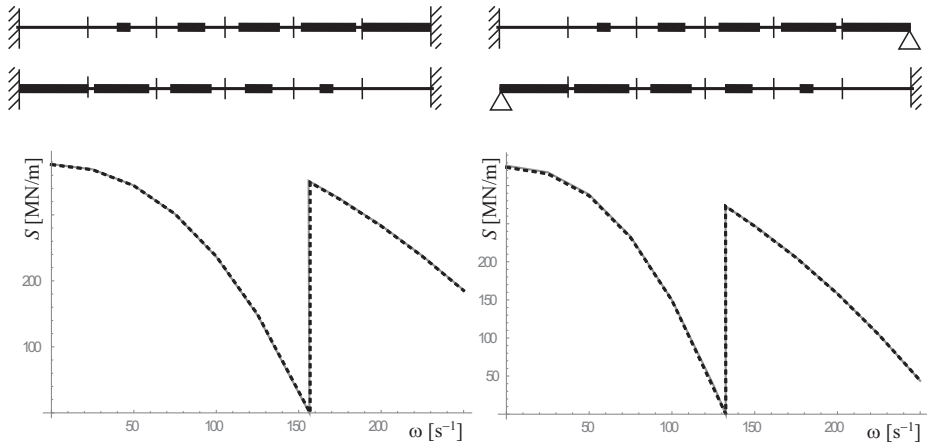


Fig. 9. Diagram $S(\omega)$ for the heterogeneous bands oriented in opposite directions:

..... lower bands, — upper bands

It has to be also emphasized that the results presented in Fig. 9 confirm the engineer's intuition – due to the assumed support conditions the bands of the left pair should be characterized by higher static critical buckling force and natural frequency for zero compressing force than the bands from the right pair.

7.5. COMPARATIVE DIAGRAMS

Fig. 10 presents the variability of the static critical buckling force S_{cr} as well as the natural frequency ω_0 for zero compressing force in the dependence on the cell number N and heterogeneity coefficients δ , r , κ . With reference to the dependence on the heterogeneity coefficients, it results from the diagrams that:

- the critical buckling force does not depend on changes of the mass (the coefficient r), whereas the natural frequency decreases if the force increases;
- both the critical buckling force and the natural frequency increase if the band stiffness (the coefficient δ) increases;
- if the subsoil stiffness (the coefficient κ) increases, then the critical buckling force and the natural frequency increase too, but the influence of the subsoil stiffness is significantly weaker than the influence of the band stiffness.

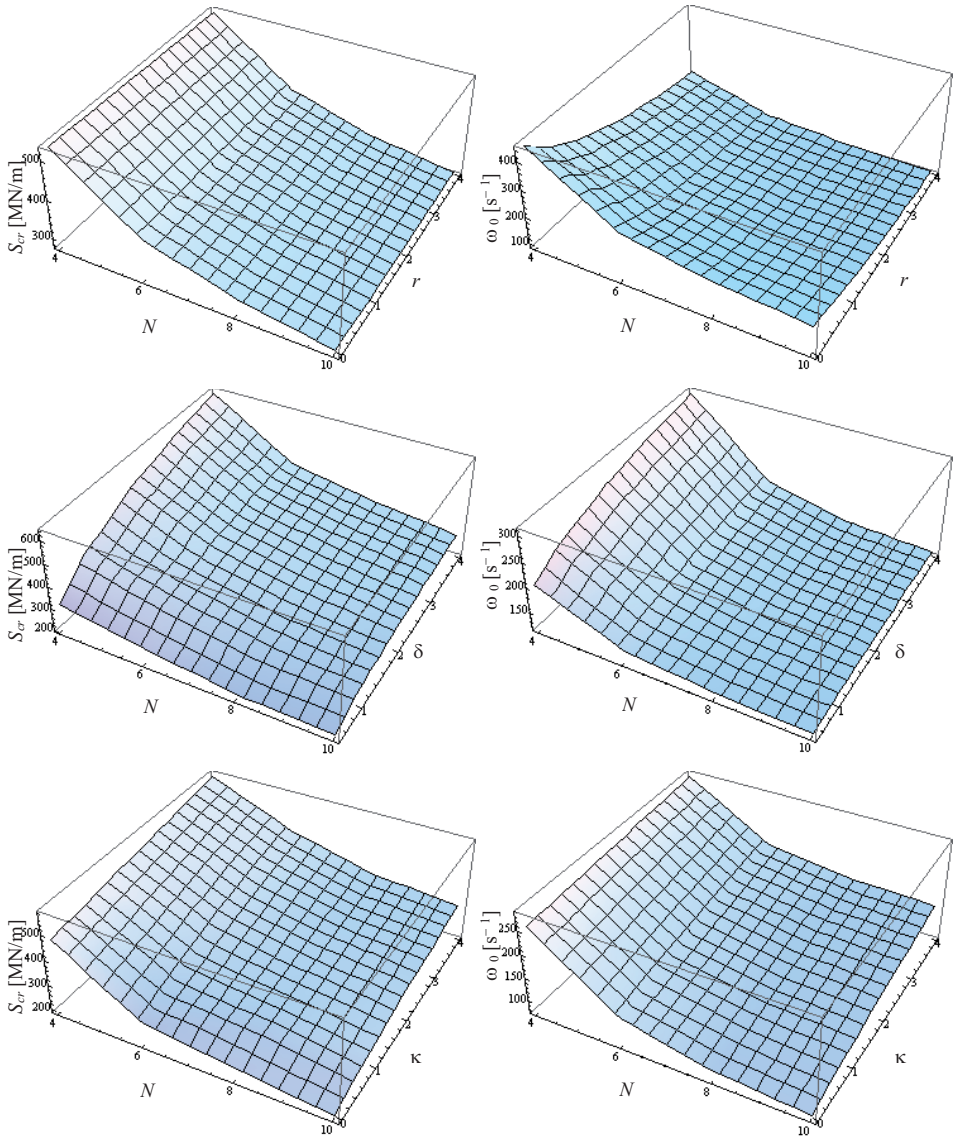


Fig. 10. Dependences of S_{cr} and ω_0 on the cell number N and heterogeneity coefficients r , δ and κ

With reference to the dependence on the cell number N , as first it must be emphasized that in the model being presented the band length L is being changed through the change of the cell number N , wherein all cells have the same length l . Therefore both the critical buckling force and the natural frequency decrease if the cell number N , i.e. the band length, increases. If one assumed that the band

length L is constant, then the changes of the cell number N would not affect the S and ω – as it was the fact in Example 3.

8. CONCLUSIONS

The presented method of modeling of micro-nonhomogeneous plate bands bases on a classical displacement method and allows to obtain in a relatively fast way, with requested accuracy, the value of the critical buckling force or natural frequency by any change of the cell length l and the parameters, characterizing: the inclusion stiffness in relation to the matrix stiffness (δ), the inclusion unit mass in relation to the matrix unit mass (r), the subsoil stiffness under the inclusion to the subsoil stiffness under the matrix (κ).

All tests performed in aim to check the correctness of the algorithm confirmed the engineer's intuition and the theoretical dependences. Namely, it has been proved that:

- the dependences of the critical buckling force (S_{cr}) and the natural frequency (ω_0) on the cell number (N) and material parameters (δ, r, κ) comply with the theory,
- the passage to the homogeneous band without subsoil (assumption $\delta = r = 1, k = 0$) gives the same results as those obtained for homogeneous beams if the beam stiffness is replaced by the plate stiffness,
- the algorithm does not show differences if the global coordinate system is reversed, i.e. it does not matter if the beginning of the band is assumed at its left or right edge (but one has to remember that the reference stiffness D and heterogeneity coefficients δ, r, κ will change),
- if the bands with the same length are calculated, the cell number N does not matter – along with the increase of this number only the accuracy of results increases (the force S_{cr} and frequency ω_0).

The above conclusions prove the correctness of the created computational algorithm. This algorithm can be also used to calculate the stability and vibrations of beams with heterogeneity along their length, whereas the cell stiffness matrix – to construct an appropriate finite element in FEM. A similar algorithm also concerns plate bands (or beams) where the inclusion stiffness varies not proportionally to a consecutive cell number j but according to any function – it only demands to choose fraction coefficients $\xi_1^{[j]}, \xi_2^{[j]}$ (formulas 2.1) in a proper way.

REFERENCES

- [1] Z. Kączkowski, *Płyty. Obliczenia statyczne*. Arkady, Warszawa 2000.
- [2] G. Jemielita, Solutions to the problems of mechanics of non-homogeneous beams and plates. In: K. Wilmański (ed.), *Mathematical methods in continuum mechanics*, Technical University of Łódź, 383-402, 2011.
- [3] W. Szcześniak, Wpływ dwuparametrowego podłoża sprężystego na drgania własne płyty o średniej grubości, *Rozprawy Inżynierskie*, 37(1), 87-115, 1989.
- [4] G. Jemielita, Z. Kozyra, Statics of beam with arbitrary stiffness resting on a variable, unidirectional, two-parameter foundation, *Theoretical Foundations of Civil Engineering, Polish-Ukrainian-Lithuanian Transactions*, Warsaw, 143-150, 2010.
- [5] M. Chalecki, G. Jemielita, Free vibrations of micro-non-homogeneous plate band, *Scientific Review Engineering and Environmental Sciences*, 23, 317-331, 2014 (in Polish).
- [6] M. Chalecki, G. Jemielita, Stability of micro-nonhomogeneous plate band, *Archives of Civil Engineering*, LXI, 91-106, 2015.
- [7] R. Solecki, J. Szymkiewicz, *Układy prętowe i powierzchniowe. Obliczenia dynamiczne*, Arkady, Warszawa 1964.
- [8] D.H.Y. Yen, S.C. Tang, On the vibration of an elastic plate on an elastic foundation, *Journal of Sound and Vibrations* 14(1), 81-89, 1971.
- [9] S.F. Bassily, S.M. Dickinson, Buckling and vibration of in-plane loaded plates treated by a unified Ritz approach, *Journal of Sound and Vibration*, 59(1), 1-14, 1978.
- [10] M.S. Cheung, A simplified finite element solution for the plates on elastic foundation, *Computers and Structures*, 8, 139-145, 1978.
- [11] J. Jędrzyśiak, Free vibrations of micro-heterogeneous thin plate band. In: G. Jemielita (ed.), *Modelling of Engineering Structures and Constructions*, Warsaw University of Life Sciences (SGGW), 133-139, 2014 (in Polish).
- [12] E. Wierzbicki, D. Kula, M. Mazewska, On Fourier realization of tolerance modelling of heat flow problems in simple periodic composites. In: G. Jemielita (ed.), *Modelling of Engineering Structures and Constructions*, Warsaw University of Life Sciences (SGGW), 253-66, 2014 (in Polish).
- [13] B. Michalak, Stability of elastic slightly wrinkled plates, *Acta Mechanica*, 130, 111-119, 1998.
- [14] E. Baron, On a certain model of uniperiodic medium thickness plates subjected to initial stresses, *Journal of Theoretical and Applied Mechanics*, 43, 93-110, 2005.
- [15] J. Rychlewska, Cz. Woźniak, M. Woźniak, Modelling of functionally graded laminates revisited, *Electronic Journal of Polish Agricultural Universities*, 9(2), #06, 2006.
- [16] J. Jędrzyśiak, On stability of thin periodic plates, *European Journal of Mechanics - A/Solids*, 19, 487-502, 2000.
- [17] J. Jędrzyśiak, Dynamic of thin periodic plates resting on a periodically non-homogeneous Winkler foundation, *Archive of Applied Mechanics*, 69, 1999.
- [18] B. Michalak, Vibrations of plates with initial geometrical imperfections interacting with periodic elastic foundation, *Archive of Applied Mechanics*, 70, 2000.
- [19] J. Jędrzyśiak, A. Paś, Vibrations of medium thickness homogeneous plates resting on a periodic Winkler subsoil. In: *Selected Topics in the Mechanics of Inhomogeneous Media*, Cz. Woźniak (ed.), R. Świtka, M. Kuczma, Zielona Góra, 133-146, 2006.

- [20] J. Jędrzyński, Application of the tolerance averaging method to analysis of dynamical stability of thin periodic plates, *Journal of Theoretical and Applied Mechanics*, 42(2), PSTAM (PTMTS), 357-379, 2004.
- [21] B. Michalak, Stability of elastic slightly wrinkled plates interacting with an elastic subsoil, *Engineering Transactions*, 47, 269-283, 1999.
- [22] Z. Naniewicz, On the homogenized elasticity with microlocal parameters, *Bulletin of Polish Academy of Sciences, Technical Sciences*, 35, 399-409, 1987.
- [23] T. Lewiński, On the interrelation between microlocal parameter and homogenization approaches to the periodic elastic solids method of modelling solids, *Bulletin of Polish Academy of Sciences, Technical Sciences*, 35, 383-391, 1987.
- [24] T. Lewiński, Homogenizing stiffnesses of plates with periodic structure, *International Journal of Solids and Structures*, 29(3), 1992.
- [25] T. Lewiński, Effective stiffnesses of transversely non-homogeneous plates with unidirectional periodic structure, *International Journal of Solids and Structures*, 32 (22), 1995.

LIST OF FIGURES:

Fig. 1. Plate band having a microstructure and resting on elastic subsoil

Rys. 1. Pasma płytowe z mikrostrukturą, spoczywające na sprężystym podłożu

Fig. 2. Dimensions of a cell

Rys. 2. Wymiary komórki

Fig. 3. Model of the band element having a number $[j]$

Rys. 3. Model elementu pasma o numerze $[j]$

Fig. 4. Schematic cross-section of the plate band

Rys. 4. Schematyczny przekrój poprzeczny pasma płytowego

Fig. 5. Diagram $S(\omega)$ for a homogeneous band: a) without subsoil, b) with subsoil

Rys. 5. Wykres $S(\omega)$ dla pasma jednorodnego: a) bez podłoża, b) z podłożem

Fig. 6. Diagram $S(\omega)$ for the heterogeneous band with subsoil: a) $N = 8$, b) $N = 10$

Rys. 6. Wykres $S(\omega)$ dla pasma niejednorodnego: a) $N = 8$, b) $N = 10$

Fig. 7. Diagram $S(\omega)$ for the homogeneous band without subsoil: a) with both edges hinged, b) with the one edge clamped and the other hinged

Rys. 7. Wykres $S(\omega)$ dla pasma jednorodnego bez podłoża: a) z obustronnym utwierdzeniem, b) z utwierdzeniem po jednej stronie i podporą przegubową po drugiej

Fig. 8. Diagram $S(\omega)$ for the heterogeneous bands having the same length

Rys. 8. Wykres $S(\omega)$ dla pasm niejednorodnych o tej samej długości

Fig. 9. Diagram $S(\omega)$ for the heterogeneous bands oriented in opposite directions: lower bands,
 — upper bands

Rys. 9. Wykres $S(\omega)$ dla pasm niejednorodnych ustawionych w przeciwnych kierunkach: pasma dolne, — pasma górne

Fig. 10. Dependences of S_{cr} and ω_0 on the cell number N and heterogeneity coefficients r , δ and κ

Rys. 10. Zależności S_{cr} i ω_0 od liczby komórek N i współczynników niejednorodności r , δ and κ

STATECZNOŚĆ I DRGANIA MIKRONIEJEDNORODNEGO PASMA PŁYTOWEGO SPOCZYWAJĄCEGO NA PODŁOŻU SPRĘŻYSTYM

Słowa kluczowe: pasmo płytowe, częstość drgań własnych, wyboczenie, podłoże sprężyste, metoda przemieszczeń

STRESZCZENIE:

W pracy przedstawiono sposób obliczania częstości drgań własnych i wyznaczania wartości sił krytycznych mikroniejednorodnego pasma płytowego o dowolnych warunkach brzegowych, spoczywającego na niejednorodnym podłożu sprężystym. Pasma składa się z N części – komórek, zwanych elementami, o stałej szerokości $l = L/N$. Każdy element pasmowy składa się z trzech części – subelementów o zmiennych szerokościach. Dwie z nich są osnową, trzecia zaś wtrąceniem symetrycznie położonym względem osnowy. Każdy element pasmowy składa się z dwóch izotropowych materiałów. Pasma osnowy i wtrącenia mają pewne sztywności i masy na jednostkę powierzchni oraz spoczywają na podłożu o pewnej sztywności. Do wyznaczenia częstości drgań własnych i wartości krytycznych zastosowano metodę przemieszczeń. Zbudowano macierz sztywności dowolnego elementu pasmowego, a następnie macierz sztywności pasma. Ułożono odpowiedni program na wyznaczenie częstości drgań własnych i sił krytycznych ze względu na wyboczenie. Wykonano szereg testów sprawdzających działanie programu i podano szereg przykładów obliczeniowych.

Received: 31.08.2020, Revised: 22.10.2020